*Journal of Statistical Physics, Vol. 127, No. 5, June 2007 (© 2007)*
DOI: 10.1007/s10955-007-9311-3

# Critical and Compensation Temperatures of the Ising Bilayer System Consisting of Spin-1/2 and Spin-1 Atoms

**E. Albayrak[1], T. Bulut[1], and S. Yilmaz[1]**

*Received October 31, 2006; accepted February 22, 2007*
*Published Online: April 3, 2007*

The critical and compensation temperatures of the bilayer Bethe lattices with one of the layers having only spin-1/2 atoms and the other having only spin-1 atoms placed symmetrically are studied by using exact recursion relations in a pairwise approach. The Hamiltonian of the model consist of the bilinear intralayer coupling constants of the two layers $J_1$ and $J_2$ for the interactions of the atoms in layers with spin-1/2 and spin-1, respectively, and the bilinear interlayer coupling constant $J_3$ between the adjacent atoms with spin-1/2 and spin-1 of the layers. After obtaining the ground state phase diagram with $J_1 > 0$, the variations of the order-parameters and the free energy are investigated to obtain the phase diagram of the model by considering only the ferromagnetic ordering of the layers, i.e. $J_1 > 0$ and $J_2 > 0$, and ferromagnetic or antiferromagnetic ordering of the adjacent spins of the layers, $J_3 > 0$ or $J_3 < 0$, respectively. It was found that the system presents both second- and first-order phase transitions and, tricritical points. The compensation temperatures was also observed for the appropriate values of the system parameters.

**KEY WORDS:** tricritical, compensation, layer, Bethe lattice, Recursion relations, spin-1/2, spin-1

**PACS**: 05.50.+q; 05.70.Fh; 64.60.Cn; 75.10.Hk

## 1. INTRODUCTION

In the recent years, in addition to one layer systems, the study of magnetic thin films consisting of various magnetic layered structures or superlattices has been receiving intense attention for both theoretical and experimental reasons.(1) These

[1] Department of Physics, Erciyes University, 38039, Kayseri, Turkey;
e-mail: albayrak@erciyes.edu.tr

materials are made up with multiple layers of different magnetic substances, thus there is a high potential for technological advances in information storage and retrieval and in synthesis of new magnets for a variety of applications.[2] They also present some interesting novel magnetic properties such as giant magnetoresistance,[3] surface magnetic anisotropy,[4] enhanced surface magnetic moment[5] and surface magnetoelastic coupling.[6]

Maybe the most studied multilayer system is the one with spin-1/2 and which was considered by using different techniques such as; effective field theory (EFT),[7] EFT based on a probability distribution technique that accounts for the self-correlation function,[8] linear cluster approximation (LCA),[9] the finite cluster approximation (FCA),[10] where in the first reference the results were also presented in a mean field theory (MFT),[11] Monte Carlo (MC) simulations,[12] Bethe-lattice approach (BLA),[13] Husimi tree approximation (HTA)[14] and on the Bethe lattice (BL) by using exact recursion equations.[15]

The next highest spin system is the spin-1 and which was also considered in the study of the multilayer systems, i.e. with MFT,[16] in the cluster variation method in the pair approximation (CVMPA), with MC simulation,[18] and on BL with and without crystal field effects,[19] respectively. We should mention that there are also some other works with higher spins which also include the multilayered systems.

In addition, the molecular-based magnetic materials with spontaneous magnetic moments are of great interest for their potential applications such as in thermomagnetic recording and in devices[20] and it is believed that ferrimagnetic ordering plays a crucial role in some of these materials. Therefore, the synthesis of new ferrimagnetic materials is an active field in material science. The ferrimagnetic materials consist of two unequal magnetic moments, i.e. a bipartite lattice with spin-$\sigma_A$ and spin-$\sigma_B$ with $\sigma_A \neq \sigma_B$, which interact antiferromagnetically, therefore, their moments do not cancel each other at low temperatures except at the compensation temperatures. The existence of compensation temperatures in ferrimagnets has an interesting application such as the magneto-optical recording.[21]

A variety of configurations of spins on a bilayer Ising model system with spin-1/2 on one layer and a higher spin on another has been attracting a great deal of attention also: A ferromagnetic amorphous bilayer system consisting of two monolayers (A and B) with different spins ($S_A = 1/2$ and $S_B = 1/2, 1$) and different interaction constants coupled together with an interlayer coupling was studied by using the EFT.[22] The critical temperature and the layer longitudinal magnetizations of a ferromagnetic or ferrimagnetic mixed Ising bilayer system with both spin-1/2 and spin-1 (or spin-3/2) in a crystal field were investigated by using EFT with a probability distribution technique.[23] The ferromagnetic or ferrimagnetic bilayer system consisting of two magnetic monolayers (A and B) with

different spins ($S_A = 1/2$ and $S_B = 1, 3/2$) and different interaction constants coupled together in a transverse crystal field were studied within the framework of EFT with correlations.[24] The differential operator technique was applied in studying the ferrimagnetic bilayer system with biaxial crystal field within the framework of EFT.[25] A ferrimagnetic bilayer system consisting of spin-1/2 and spin-3/2 Ising layers in an applied transverse field were examined by the use of EFT.[26] A ferromagnetic amorphous bilayer system consisting of two magnetic monolayers with spin-1/2 and spin-3/2 and different interaction constants coupled together with interlayer coupling was studied by the use of the EFT.[27] Transition temperatures of a bilayer system with $(A)_2(A_pB_{1-p})_1(B)_2$ consisting periodically of two layers of spin-1/2 A atoms, two layers of spin-3/2 atoms and an interface with alloying type $(A_pB_{1-p})$ disorder were examined by using the EFT.[28] The effects of an applied transverse magnetic field on magnetic properties in a ferrimagnetic bilayer system with disordered interfaces consisting of spin-1/2 and spin-3/2 atoms were investigated with the use of the MFT.[29] The magnetic properties of a ferromagnetic bilayer system consisting of spin-1/2 and spin-3/2 Ising layers in an applied transverse field were examined by the use of EFT.[30] The spin configurations in the absence of an external magnetic field have been systematically investigated for a magnetic bilayer system of two ferromagnetic layers separated by a non-magnetic layer with exchange interlayer coupling.[31]

In this paper, the bilayer model with one of the layers containing only spin-1/2 atoms and the other having only spin-1 atoms, each of them are allowed to interact ferromagnetically with bilinear intralayer interactions $J_1$ and $J_2$, respectively, and with bilinear interlayer interaction $J_3$ between the layers either ferromagnetic or antiferromagnetic interactions, is studied by using the exact recursion relations in a pairwise approach (meaning that one spin from the upper layer with spin-1/2 and whose adjacent nearest-neighbor spin with spin-1 from the lower layer form a pair) on the Bethe lattice.[32] Besides the ground state phase diagram, the phase diagrams of the model are also calculated by studying the variations of the order-parameters and the free energy of the system.

We have organized the rest of the paper as follows. In Sec. 2, bilayer Ising model is introduced and then the ground state phase diagram is obtained and discussed. In Sec. 3 we have obtained the order-parameters and free energy of the system in terms of the recursion relations exactly. In Sec. 4 we have presented the thermal and $J_3/J_1$ change of the total and staggered magnetizations of the two layers and also the spin-spin correlation function between the nearest-neighbor spins of the adjacent layers, thus the phase diagram of the model is obtained on the $(kT/J_1, J_3/J_1)$ plane for given values of $J_2/J_1$ and $q$. Finally in the last section we give a brief summary and discussions.

## 2. BILAYER BETHE LATTICE AND ITS GROUND STATES

In the bilayer version of the Bethe lattice,[19,32] each spin far from the boundary sites, i.e. deep inside, has $q$ nearest-neighbors (NN) from its own layer and one adjacent NN from the other layer, therefore, in total each spin has $q+1$ neighbors. Thus, the Hamiltonian including all the NN bilinear spin interactions on the bilayer Bethe lattice away from the boundaries may be written as

$$\mathcal{H} = -J_1 \sum_{\langle ij \rangle} S_i S_j - J_2 \sum_{\langle i'j' \rangle} \sigma_{i'} \sigma_{j'} - J_3 \sum_{\langle ii' \rangle} S_i \sigma_{i'}, \tag{1}$$

where $S_i$ refers to spin-1/2 with values $\pm 1/2$ on layer $G_1$ and $\sigma_{i'}$ refers to spin-1 with the values $\pm 1$ and 0 on layer $G_2$, $J_1$ and $J_2$ are the intralayer bilinear interactions of the layers and the first and second summation runs over all sites of $G_1$ and $G_2$, respectively. $J_3$ is the interlayer bilinear interaction of the NN spins between the layers $G_1$ and $G_2$, thus the third summation runs over all the adjacent neighboring sites of $G_1$ and $G_2$.

In order to obtain an exact formulation of the model, one needs to introduce the order-parameters. It should be mentioned that in the thermodynamic limit, i.e. the number of shells go to infinity, all sites deep inside the bilayer BL with same kinds of spins are equivalent. Therefore, one can pick two adjacent NN spins, i.e. spin-1/2 from $G_1$ and spin-1 from $G_2$, as the central pair. As a result, the spin-1/2 of the central pair from $G_1$ and spin-1 of the central pair from $G_2$ have the magnetizations defined as

$$m_1 = \langle S_0 \rangle \qquad \text{and} \qquad m_2 = \langle \sigma_{0'} \rangle \tag{2}$$

our first two order-parameters, respectively, and where $\langle ... \rangle$ refers to the usual thermal average. Instead of these order-parameters, without loss of generality, it is much appropriate to use the total magnetization $m$ and the staggered magnetization $\eta$

$$m = \frac{1}{2}(m_1 + m_2), \quad \eta = \frac{1}{2}(m_1 - m_2) \tag{3}$$

as two of the order-parameters of the model. The last order-parameter is the spin-spin correlation function of the adjacent NN spins in the central pair and defined as

$$\rho = \langle S_0 \sigma_{0'} \rangle - \langle S_0 \rangle \langle \sigma_{0'} \rangle \tag{4}$$

In order to determine the stable solutions of the model, first we have obtained the ground state phase diagram for $J_1 > 0$, ferromagnetic interaction in layer $G_1$, on the $(J_2/|J_1|, J_3/q|J_1|)$ plane. Thus, the ground-state energy in units of $|J_1|$ may be described by the following Hamiltonian:

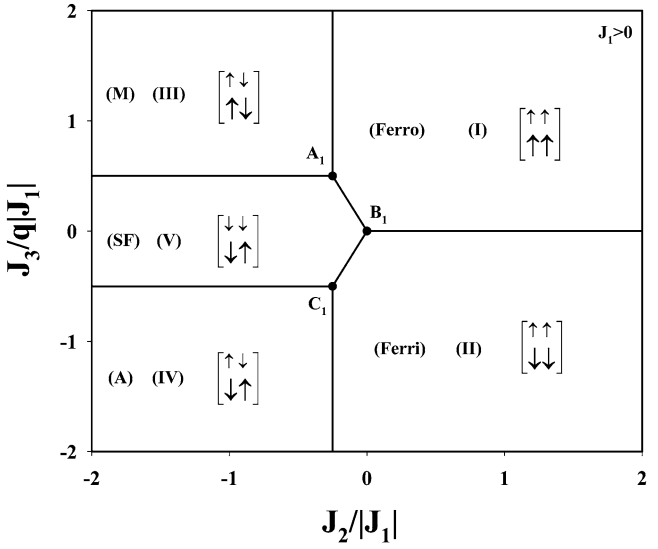


**Fig. 1.** The ground state phase diagram of the bilayer spin-1/2 and spin-1 Ising model for $J_1 > 0$. Five different phases depending on the spin configurations are indicated as: ferromagnetic (Ferro), ferrimagnetic (Ferri), mixed (M), antiferromagnetic (A) and surface ferromagnetic (SF), which are all separated by multiphase lines.

$$\frac{E}{q|J_1|} = -\sum_{\langle \text{plaq} \rangle} \left[ \frac{J_1}{|J_1|} S_i S_j + \frac{J_2}{|J_1|} \sigma_{i'} \sigma_{j'} + \frac{J_3}{q|J_1|} (S_i \sigma_{i'} + S_j \sigma_{j'}) \right]. \tag{5}$$

Here the summation goes over all the plaquette and each plaquette consists of four nearest-neighbor pair of the two-layer system with one pair $\langle ij \rangle$ with spin-1/2 only on layer $G_1$, one pair $\langle i'j' \rangle$ with spin-1 only on layer $G_2$, and two pairs $\langle ii' \rangle$ and $\langle jj' \rangle$ connecting layers $G_1$ and $G_2$ between the two spin-1/2 and spin-1 pairs only.

The ground state phase diagram, Fig. 1, is obtained by comparing the values of the energy $E/q|J_1|$ for different spin configurations and then the ground state configurations are the ones with the lowest energy for given values of $J_2/|J_1|$ and $J_3/q|J_1|$. As a result, we have obtained five different types of ground state configurations with the following values of the order-parameters $(m, \eta, \rho)$:

| | | | | |
|---|---|---|---|---|
| **I**. | Ferromagnetic (Ferro) | $m = \pm 3/4,$ | $\eta = \mp 1/4,$ | $\rho = 0,$ |
| **II**. | Ferrimagnetic (Ferri) | $m = \pm 1/4,$ | $\eta = \mp 3/4,$ | $\rho = 0,$ |
| **III**. | Mixed (M) | $m = 0,$ | $\eta = 0,$ | $\rho = 1/2,$ |
| **IV**. | Antiferromagnetic (A) | $m = 0,$ | $\eta = 0,$ | $\rho = -1/2,$ |
| **V**. | Surface Ferromagnetic (SF) | $m = \pm 1/4,$ | $\eta = \pm 1/4,$ | $\rho = 0.$ |

As shown in the figures the coordinates $(J_2/|J_1|, J_3/q|J_1|)$ of the multiphase points are

$$A_1 \to (-0.25, 0.5), \quad B_1 \to (0, 0),$$
$$C_1 \to (-0.25, -0.5), \quad \text{for } J_1 > 0. \tag{6}$$

Phase I represents the usual ferromagnetic (Ferro) ordering, i.e the ordering in layers $G_1$ and $G_2$ and between them are totally ferromagnetic. Phase II presents ferromagnetic ordering in $G_1$ and $G_2$, separately, but magnetizations in $G_1$ and $G_2$ are antiparallel, that is the interlayer ordering is antiferromagnetic type. The magnetizations of the two layers do not cancel each other, i.e. spin-1/2 and spin-1, so this phase is called as the ferrimagnetic (Ferri) phase. Phase III shows antiferromagnetic ordering (A) in both layers ($m_1 = m_2 = 0$) where interlayer ordering is ferromagnetic type, therefore as a whole the system is in a mixed phase (M). Phase IV illustrates the totally antiferromagnetic (A) ordering, i.e. the interaction in both layers and in between the layers are antiferromagnetic. Phase V represents the ferromagnetic ordering which is equivalent to the case that the ground state of one layer is ferromagnetic and the ground state of another layer is antiferromagnetic, thus called as the surface magnetic phase (SF). These phases are indicated with $(S_0, S_1)$ and $(\sigma_{0'}, \sigma_{1'})$ pairs in the figures for layers $G_1$ and $G_2$ with small and big arrows, respectively.

The ground state phase diagram of this spin-1/2 and spin-1 bilayer system is qualitatively similar with the ground state phase diagrams of the bilayer system with single type spins, i.e. spin-1/2, spin-1 and spin-3/2 in Ref. 32, respectively. But the values of the multiphase points of this work are different when compared with the corresponding values for the spin-1/2, spin-1 and spin-3/2 bilayer systems which all have the same values.

## 3. THE CALCULATIONS OF THE ORDER-PARAMETERS AND THE FREE ENERGY OF THE BILAYER SYSTEM

In order to obtain the order-parameters and the free energy in terms of the recursion relations on the bilayer Bethe lattice, first we have to calculate the partition function of the system by using the Ising Hamiltonian given in Eq. (1). It is assumed that adjacent NN spins of $G_1$ and $G_2$ are considered as pairs each of which has one spin-1/2 and one spin-1 atoms. The first pair deep inside the bilayer lattice is called the central pair which forms the first-generation spins. This central pair of spins connected by $q$ NN spin pairs, i.e. coordination number, which forms the second-generation spins. Each pair of spins in the second-generation is joined to $(q-1)$ NN's. Therefore, in total the second-generation has $q(q-1)$ NN's which form the third-generation and so on to infinity.[32] As a result each spin has $(q+1)$ NN spins, $q$ spins from the layer it belongs to, i.e. with

same type of spin, and one from the adjacent layer, i.e. with the other type of spin.

Let us start with the partition function defined as

$$Z = \sum_{\text{All Config.}} e^{-\beta\mathcal{H}} = \sum_{Spc} P(Spc), \tag{7}$$

where $P(Spc)$, $Spc$ refers to the spin configurations, can be thought of as an unnormalized probability distribution. Starting from the central pair of spins on the Bethe lattice, one reaches to one of the pair spins at the boundary by moving on any path of the tree, which is made up with separate branches connecting each of the pair of spins, therefore, for the full formulation one has to define the partition function for each of these separate branches named as $g_n(S, \sigma)$. It should be mentioned that each spin with spin-1/2 can take the values $\pm 1/2$ and with spin-1 can take the values $\pm 1$ and 0, therefore, for the bilayer model we have to define six $g_n(S, \sigma)$ functions for $2 \times 3 = 6$ configurations for each pair of spins at their sites. Thus in this pairwise approach,[32] five exact recursion relations are defined as the ratios of these partition functions of the separate branches on the bilayer Bethe lattice as

$$A_n = \frac{g_n\left(\frac{1}{2}, 1\right)}{g_n\left(-\frac{1}{2}, 0\right)}, \quad B_n = \frac{g_n\left(\frac{1}{2}, 0\right)}{g_n\left(-\frac{1}{2}, 0\right)}, \quad C_n = \frac{g_n\left(\frac{1}{2}, -1\right)}{g_n\left(-\frac{1}{2}, 0\right)},$$
$$D_n = \frac{g_n\left(-\frac{1}{2}, 1\right)}{g_n\left(-\frac{1}{2}, 0\right)}, \quad E_n = \frac{g_n\left(-\frac{1}{2}, -1\right)}{g_n\left(-\frac{1}{2}, 0\right)}, \tag{8}$$

Note that each recursion relation is a function of the recursion relations for the NN shell with $(n-1)$, therefore, these equations are totally nonlinear in their nature, thus in order to obtain their numerical values for given system parameters numerical methods have to be carried out. We should also mention that the choice of what ratios of these $g_n(S, \sigma)$ functions is to be taken is totally arbitrary. Hence the explicit formulations of the recursion relations are

$$\begin{aligned}
A_n &= \left[e^{\beta(J_1/4+J_2+J_3/2)}A_{n-1}^{q-1} + e^{\beta(J_1/4)}B_{n-1}^{q-1} + e^{\beta(J_1/4-J_2-J_3/2)}C_{n-1}^{q-1}\right. \\
&\quad \left. + e^{\beta(-J_1/4+J_2-J_3/2)}D_{n-1}^{q-1} + e^{\beta(-J_1/4-J_2+J_3/2)}E_{n-1}^{q-1} + e^{\beta(-J_1/4)}\right]\Big/\Delta_1, \\
B_n &= \left[e^{\beta(J_1/4+J_3/2)}A_{n-1}^{q-1} + e^{\beta(J_1/4)}B_{n-1}^{q-1} + e^{\beta(J_1/4-J_3/2)}C_{n-1}^{q-1}\right. \\
&\quad \left. + e^{\beta(-J_1/4-J_3/2)}D_{n-1}^{q-1} + e^{\beta(-J_1/4+J_3/2)}E_{n-1}^{q-1} + e^{\beta(-J_1/4)}\right]\Big/\Delta_1, \\
C_n &= \left[e^{\beta(J_1/4-J_2+J_3/2)}A_{n-1}^{q-1} + e^{\beta(J_1/4)}B_{n-1}^{q-1} + e^{\beta(J_1/4+J_2-J_3/2)}C_{n-1}^{q-1}\right. \\
&\quad \left. + e^{\beta(-J_1/4-J_2-J_3/2)}D_{n-1}^{q-1} + e^{\beta(-J_1/4+J_2+J_3/2)}E_{n-1}^{q-1} + e^{\beta(-J_1/4)}\right]\Big/\Delta_1,
\end{aligned}$$

$$D_n = \left[e^{\beta(-J_1/4+J_2+J_3/2)}A_{n-1}^{q-1} + e^{\beta(-J_1/4)}B_{n-1}^{q-1} + e^{\beta(-J_1/4-J_2-J_3/2)}C_{n-1}^{q-1} + e^{\beta(J_1/4+J_2-J_3/2)}D_{n-1}^{q-1} + e^{\beta(J_1/4-J_2+J_3/2)}E_{n-1}^{q-1} + e^{\beta(J_1/4)}\right]\Big/\triangle_1,$$

$$E_n = \left[e^{\beta(-J_1/4-J_2+J_3/2)}A_{n-1}^{q-1} + e^{\beta(-J_1/4)}B_{n-1}^{q-1} + e^{\beta(-J_1/4+J_2-J_3/2)}C_{n-1}^{q-1} + e^{\beta(J_1/4-J_2-J_3/2)}D_{n-1}^{q-1} + e^{\beta(J_1/4+J_2+J_3/2)}E_{n-1}^{q-1} + e^{\beta(J_1/4)}\right]\Big/\triangle_1. \quad (9)$$

In the thermodynamic limit ($n \to \infty$) these recursion relations determine the states of the system, therefore, they may be called as the equations of state. The magnetization of the central spin with spin-1/2 in layer $G_1$

$$m_1 = \langle S_0 \rangle = \left\{\frac{1}{2}e^{\beta J_3/2}A_n^q + \frac{1}{2}B_n^q + \frac{1}{2}e^{-\beta J_3/2}C_n^q - \frac{1}{2}e^{-\beta J_3/2}D_n^q - \frac{1}{2}e^{\beta J_3/2}E_n^q - \frac{1}{2}\right\}\Big/\triangle_2, \quad (10)$$

the magnetization of the spin-1 of the central pair in layer $G_2$

$$m_2 = \langle \sigma_{0'} \rangle = \left\{e^{\beta J_3/2}A_n^q - e^{-\beta J_3/2}C_n^q + e^{-\beta J_3/2}D_n^q - e^{\beta J_3/2}E_n^q\right\}\Big/\triangle_2, \quad (11)$$

and the spin-spin correlation function between the spins of central pair is expressed by

$$\rho = \langle S_0\sigma_{0'} \rangle - \langle S_0 \rangle\langle \sigma_{0'} \rangle = \left\{\frac{1}{2}e^{\beta J_3/2}A_n^q - \frac{1}{2}e^{-\beta J_3/2}C_n^q - \frac{1}{2}e^{-\beta J_3/2}D_n^q + \frac{1}{2}e^{\beta J_3/2}E_n^q\right\}\Big/\triangle_2 - m_1 m_2, \quad (12)$$

where

$$\triangle_2 = e^{\beta(J_3/2)}A_n^q + B_n^q + e^{\beta(-J_3/2)}C_n^q + e^{\beta(-J_3/2)}D_n^q + e^{\beta(J_3/2)}E_n^q + 1 \quad (13)$$

In addition to the behaviors of the order-parameters, we also need the free energy in terms of the recursion relations to obtain the phase diagrams of the model. Therefore, the free energy of the bilayer Bethe lattice is given as

$$-\beta F = \mathrm{Log}(\triangle_2) + \frac{q}{2-q}\mathrm{Log}(\triangle_1) \quad (14)$$

and which is used to find the places of the first-order phase transition temperatures and the stable solutions of the model and where

$$\triangle_1 = e^{\beta(-J_1/4+J_3/2)}A_{n-1}^{q-1} + e^{\beta(-J_1/4)}B_{n-1}^{q-1} + e^{\beta(-J_1/4-J_3/2)}C_{n-1}^{q-1} + e^{\beta(J_1/4-J_3/2)}D_{n-1}^{q-1} + e^{\beta(J_1/4+J_3/2)}E_{n-1}^{q-1} + e^{\beta(J_1/4)}. \quad (15)$$

Meanwhile, it should be reminded that in order to obtain the variations of the order-parameters and the free energy for given system parameters, first the recursion relations are calculated by using an iteration scheme for given initial values of the recursion relations, which may yield more than one solutions with different free energies, then the found values of the recursion relations are inserted into the definitions of the order-parameters and the free energy. Of course, only the solution which minimizes the free energy of the system is thermodynamically stable. The others correspond to unstable or metastable solutions. If there are two or more solutions that have the same minimum free energies, these phases coexist and the system has a first-order phase transition. In the next section, we analyze the behaviors of the order-parameters and free energy for given system parameters and as a result we obtain the phase diagrams of the model.

## 4. THE THERMAL CHANGE OF THE ORDER-PARAMETERS AND THE PHASE DIAGRAMS

In this section, the variations of the magnetizations, spin-spin correlation function and the free energy are studied in terms of the recursion relations to obtain the phase diagrams of the model. As we have noted earlier, the calculations are carried out for only $J_1 > 0$ and $J_2 > 0$, ferromagnetic couplings in layers $G_1$ and $G_2$, and $J_3 > 0$ or $J_3 < 0$, ferromagnetic or antiferromagnetic coupling between the layers, respectively.

The definition of the second-order phase transition or Curie temperature, $T_c$, is illustrated in Fig. 2 in terms of the thermal variations of the order-parameters. The values of $J_2/J_1 = 1.0$ and $J_3/J_1 = 1.0$ are chosen corresponding to the phase (I) of the ground state. As seen $m$, $\eta$ and $\rho$ begin from 0.75, $-0.25$ and 0.0 at zero temperature and as the temperature increases they change gradually and at $T_c$, $m$ from above and $\eta$ from below go to zero where $\rho$ makes a peak at its maximum. But in the inset of the figure for $J_3/J_1 = -1.0$ corresponding to the phase (II) of the ground state in comparison with the figure for $J_3/J_1 = 1.0$, $m$ and $\eta$ exchange the roles and $\rho$ changes sign as expected.

The way to obtain the first-order phase transition temperatures, $T_t$, is illustrated in Fig. 3. For this we have plotted the order-parameters and the free energy with respect to the ratio $J_3/J_1$ for given values of the temperature, since as seen in the ground state phase diagram the positive part of the abscissa is the first-order phase line separating the phases I and II. At this temperature for $J_3/J_1 = 0$, the free energy of the system jump from phase I to phase II or vice versa. In Fig. 3a, the change of the magnetizations with respect to $J_3/J_1$ is obtained for $kT/J_1 = 0.35$, $J_2/J_1 = 1.0$ and $q = 3$. As seen $m = \pm 0.25$ and $\eta = \pm 0.75$ for $J_3/J_1 < 0$. These values of $m$ and $\eta$ continues until very close to $J_3/J_1 = 0$, where they make little peaks, and then they exchange the roles when $J_3/J_1$ changes sign. Namely, $m = \pm 0.75$ and $\eta = \pm 0.25$ for $J_3/J_1 > 0$. As seen in the insets the free energy

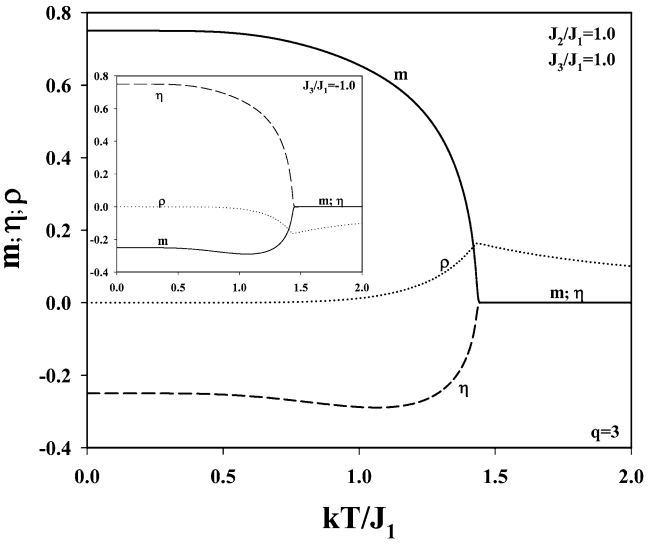


**Fig. 2.** The thermal variations of $m$, $\eta$ and $\rho$ showing the existence of the second-order phase transitions for $q = 3$, $J_2/J_1 = 1.0$ and $J_3/J_1 = 1.0$ and in the inset $J_3/J_1 = -1.0$ corresponding the (I) and (II) phases, respectively.

is discontinuous at $J_3/J_1 = 0$ and $\rho$ gives two small peaks at the two sides of $J_3/J_1 = 0$ with minimum and maximum, respectively. At $kT/J_1 = 1.64$ as shown in Fig. 3b for $J_2/J_1 = 1.0$, the system gives only second-order phase transitions. Where for $J_3/J_1 = -20.0$, $m$'s start from $\pm 0.2360$ and $\eta$'s start from $\pm 0.7083$. As $J_3/J_1$ is increased from left, $m$ and $\eta$ decreases until the $J_3/J_1 = -2.28$, where they are zero, indicating the second-order phase transition. At this value $\rho$ shows its first peak as a minimum. The region enclosed by the wings of the staggered magnetization corresponds to phase II, i.e. the ferrimagnetic phase. The zero values of $m$ and $\eta$ continues until $J_3/J_1 = 2.28$, but $\rho$ increases from its minimum to its maximum, i.e. to its second peak at $J_3/J_1 = 2.28$, in this paramagnetic region. At $J_3/J_1 = 2.28$, $m$ and $\eta$ again exchange the roles, therefore, now the region enclosed by the wings of the total magnetization corresponds to phase I, i.e. the ferromagnetic phase. As the temperature is decreased, the wings of the total and staggered magnetizations get close to each other until some critical temperature, where these two wings just touch each other at $J_3/J_1 = 0.0$, below which the system only presents first-order phase transitions as shown in Fig. 3a. Again the $J_3/J_1$ behavior of the free energy for these values are included into the figures as insets, for the first-order phase transitions the two branches of the free energy corresponding to negative and positive $J_3/J_1$ axes combine at $J_3/J_1 = 0$ in a discontinuous manner.

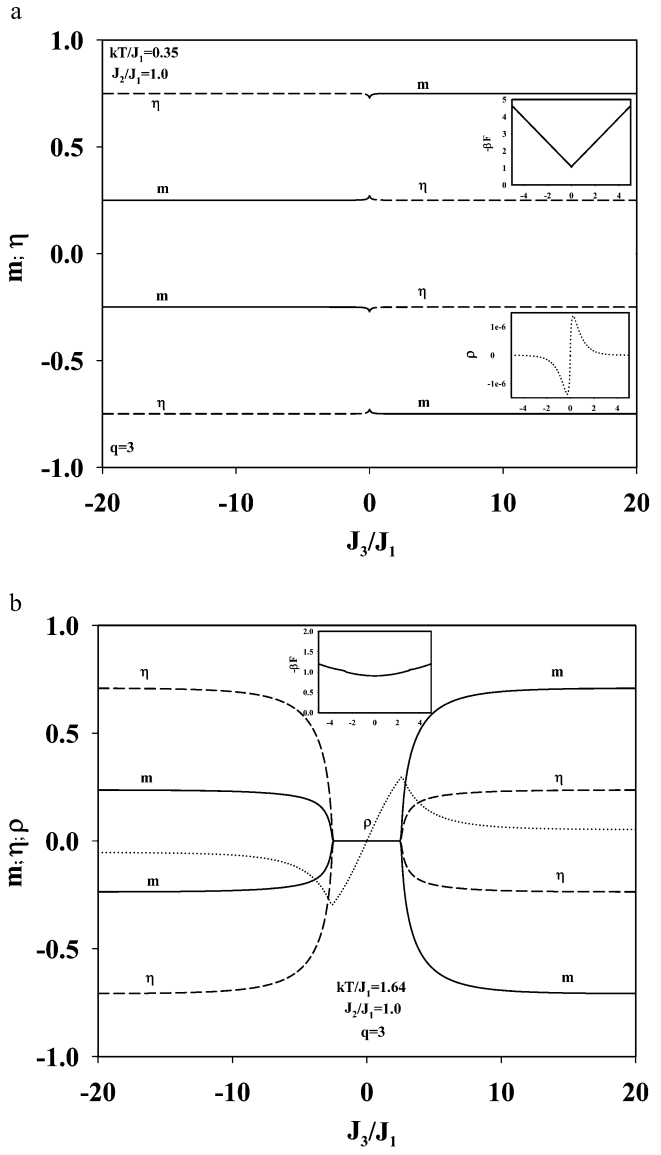


**Fig. 3.** The $J_3/J_1$ change of $m$, $\eta$ and $\rho$ for $q = 3$ and $J_2/J_1 = 1.0$ showing the way of obtaining the first-order phase transitions a- $kT/J_1 = 0.35$ and the way of obtaining the second-order phase transitions b- $kT/J_1 = 1.64$.

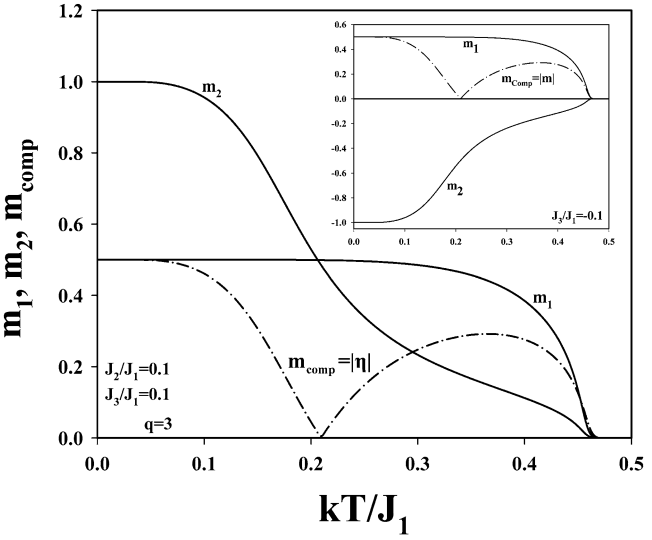


**Fig. 4.** The thermal variations of the layer magnetizations $m_1$ and $m_2$, and $m_{\text{comp}}$ as $|m|$ and $|\eta|$ corresponding to phase (II) and phase (I), respectively, for $q = 3$ and $J_2/J_1 = 0.1$ showing the existence of the compensation temperatures for $J_3/J_1 = 0.1$ and in the inset for $J_3/J_1 = -0.1$.

The existence of the compensation temperatures, the temperature at which the layer magnetizations become equal before $T_c$, is demonstrated in Fig. 4 by studying the temperature change of the magnetizations. Besides $m_1$ and $m_2$, we have also illustrated the temperature change of the absolute values of $m$ and $\eta$ corresponding to the phases (I) and (II), respectively, to see the places of the compensation temperatures clearly. The main figure was obtained for $J_2/J_1 = 0.1$, $J_3/J_1 = 0.1$ and $q = 3$ corresponding to the phase (I) and in the inset $J_3/J_1$ was set equal to $-0.1$ corresponding to phase (II). Thus the existence of only one compensation temperature is in agreement with the works including the transverse crystal field[23,24] and biaxial crystal field[25] effects, where they report finding of one compensation temperature when these effects are either on or off, but of course our work does not include any crystal field effects.

After having studied the variations of the order-parameters and the free energy, we are ready to obtain the phase diagrams of our model on the $(kT/J_1, J_3/J_1)$ plane for given values of $J_2/J_1$ and $q$. In the phase diagrams, Figs. 5 and 6, the second- and first-order lines and the lines of the compensation temperatures are indicated with solid, dashed and gray-dashed lines, respectively, and the filled circles indicate the tricritical points, $T_{c_q}$, $q$ is the corresponding coordination number. The different phase regions indicated with (Ferro), (P) and (Ferri) corresponding to ferromagnetic, paramagnetic and ferrimagnetic phases, respectively. The phases

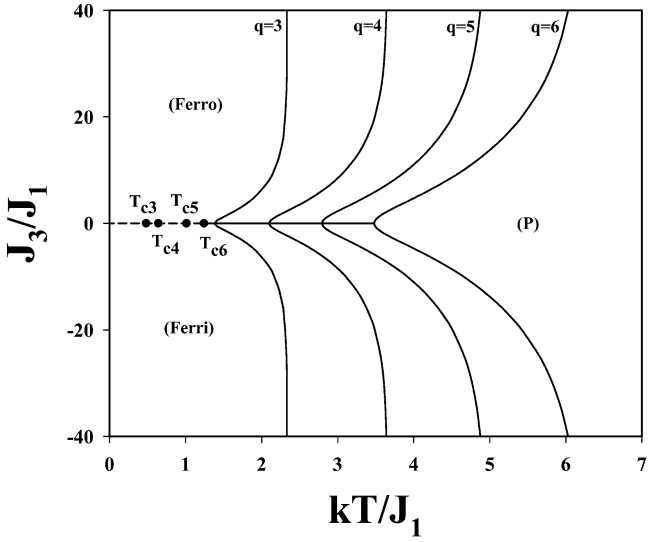


**Fig. 5.** The phase diagram of the spin-1/2 and spin-1 Ising model for the bilayer Bethe lattice on the $(kT/J_1, J_3/J_1)$ plane for $q = 3, 4, 5$ and 6. The effect of increasing the $q$ is illustrated.

(Ferro) and (Ferri) are separated with a first-order line at low temperatures which continues until the tricritical point from which second-order lines emerge for each given values of $q$ along the $J_3/J_1 = 0$ still separating (Ferro) and (Ferri) phases. These second-order lines for each $q$ continue until the temperature named as $T_{TP_q}$, where $TP$ refers to the triple point and where the phases (Ferro), (P) and (Ferri) all coexist together. At these triple point for each $q$ the second-order lines separate into two symmetrical wings, i.e. while the upper $T_c$ line separates the (Ferro) and (P) phases corresponding to $J_3/J_1 > 0$ the lower one separates the (Ferri) and (P) phases corresponding to the $J_3/J_1 < 0$.

In Fig. 5, we present the effect of increasing the coordination number $q$ in the phase diagram for $J_2/J_1 = 1.0$. The temperatures $T_{c_q} \cong 0.48$, 0.64, 1.01 and 1.24 and $T_{TP_q} \cong 1.384$, 2.098, 2.794 and 3.481 correspond to $q = 3$, 4, 5 and 6, respectively. Meanwhile in the limit $J_3/J_1 \to \pm\infty$, the second-order phase transition temperatures become constant at 2.332, 3.64, 5.02 and 6.3 for $q = 3$, 4, 5 and 6, respectively. So increasing the $q$ does not lead any qualitative changes in the phase diagram.

The effect of changing $J_2/J_1$ values was illustrated in Fig. 6 when $q = 3$ by setting $J_2/J_1 = 0.1$, 0.25, 0.5, 0.75 and 1.0. The tricritical temperatures corresponding to these values of $J_2/J_1$ are about 0.07, 0.25, 0.45, 0.47 and 0.48 respectively. It is obvious that as $J_2/J_1$ values increase towards 1.0 their tricritical point temperatures get closer to each other and the critical temperatures are seen at higher

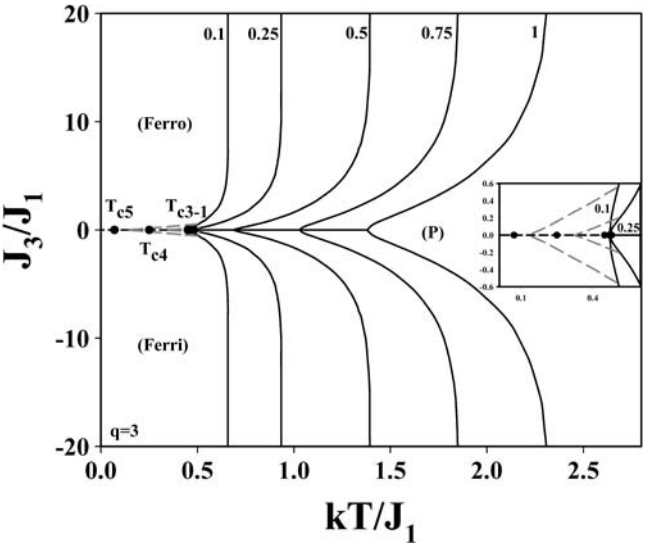


**Fig. 6.** The phase diagram of the model $J_2/J_1 = 0.1, 0.25, 0.5, 0.75$ and 1.0 for $q = 3$. The effect of changing the $J_2/J_1$ values is demonstrated.

temperatures. Namely, as $J_2/J_1$ values decrease the paramagnetic phase pushes the second-order phase transition lines towards to lower temperatures. The $T_{TP_3} \cong 0.472, 0.472, 0.694, 1.033$ and 1.384 for the $J_2/J_1$ values respectively. In addition in the limit $J_3/J_1 \to \pm\infty$, the second-order phase transition temperatures become constant at 0.7, 0.98, 1.44, 1.92 and 2.38 for $J_2/J_1 = 0.1, 0.25, 0.5, 0.75$ and 1.0, respectively. It is found that the system presents compensation temperatures for $J_2/J_1 = 0.1$ and 0.25 when $q = 3$ and none was found for $J_2/J_1 = 0.5, 0.75$ and 1.0. The compensation temperatures are found by taking the absolute values of $m$ and $\eta$ in the regions with phase (II) and phase (I), respectively. Thus for each values of $J_2/J_1$ two symmetrical branch of compensation lines emerging from the same temperature, i.e. about 0.13 and 0.328 for the corresponding $J_2/J_1 = 0.1$ and 0.25, on $J_3/J_1 = 0$ are found. As the temperature increases these branches move to higher $|J_3/J_1|$ values and eventually end on the corresponding second-order line at temperatures about 0.5 and 0.508 for $J_2/J_1 = 0.1$ and 0.25 and $J_3/J_1 = 0.55$ and 0.2, respectively. We should note that for the higher values of the coordination number the obtained phase diagrams are qualitatively similar, therefore, we have not presented their phase diagrams in here.

In concluding this section we should note that there are two theoretical works that we can compare our results with, i.e. the effect of the interlayer exchange interaction $J_{\text{inter}}$ in coupled Co/Cu/Ni trilayers was studied as motivated by the experiments,[33] where they find an overall agreement with the experimental results,

see the references there. Their phase diagrams, i.e. Fig. 3, is qualitatively similar with our phase diagrams presented here. The last work is the one which investigates the phase transitions in a bi-layer lattice gas[34] modeled analogically same with this work presents a phase diagram again quantitatively similar with our work. In their phase diagram, Fig. 3, the different phases are indicated as disorder (D), Full/Empty (FE) and strip (S) which correspond to our (P), (Ferri) and (Ferro) phases, respectively.

## 5. CONCLUSIONS

In conclusion, we have studied the bilayer spin-1/2 and spin-1 Ising model on the Bethe lattice in detail in terms of the intralayer coupling constants $J_1$ and $J_2$ of the two layers, ferromagnetic case only, interlayer coupling constant $J_3$ between the layers, ferromagnetic or antiferromagnetic, for given values of the coordination number $q$ in terms of the recursion relations. The ground state phase diagrams of the model is obtained on the $(J_2/|J_1|, J_3/q|J_1|)$ plane for $J_1 > 0$. Then, by studying the variations of the order-parameters and the free energy, the phase diagrams of the model are obtained on the $(kT/J_1, J_3/J_1)$ planes for given values of $J_2/J_1$ and coordination numbers. As a result, we have found that the system presents both first- and second-order phase transitions for all values of $q$. The first-order lines separate the two ordered phases, i.e. (Ferro) and (Ferri) phases at low temperatures which continue until the tricritical point. Between the two wings of the second order lines is the disordered phase, i.e. paramagnetic phase. It is found that the system also presents compensation temperatures for lower values of the $J_2/J_1$, i.e. when $J_2 < J_1$ the magnetization of layer $G_2$ with spin-1 can compensate the magnetization of layer $G_1$ with spin-1/2.

Since $J_3$ is the bilinear interlayer interaction between the layers $G_1$ and $G_2$, when it equals to zero the two layer Bethe lattice reduces to the two independent single layer lattices with only spin-1/2 and spin-1, respectively. When $J_3 \neq 0$, the layers can interact with each other and as seen from the ground state figures when $J_3 > 0$ the interaction is ferromagnetic type while for $J_3 < 0$ is the ferrimagnetic type. At low temperatures along the $J_3 = 0$ axis, these two phases are symmetric and, therefore, the free energy has two minimums, thus as this axis is passed, which corresponds to a sign change for $J_3$, the system jumps from one minimum to the other, therefore, a first-order phase transition is seen. As the temperature is increased the potential barrier between these two minimums of the free energy decreases and, therefore, when the system passes from (Ferro) to (Ferri) phases no extra energy is required since it is obtained from the temperature itself, now only a second-order phase transition is seen separating (Ferro) and (Ferri) phases. It should also be mentioned that these two lines merge with each other at a tricritical temperature $T_{c_q}$ as explained in the text. As the temperature is increased further, because of the competitions between the bilinear interactions and the temperature,

the paramagnetic phase is also seen. At high temperatures the bilinear interactions can not afford to hold the system in the ordered phase, the temperature causes the spins to move randomly corresponding to the paramagnetic (P) case, separating the (Ferro) and (Ferri) phases. Finally, for very high temperature only (P) phase is seen as expected. It should be mentioned that the intersections of these three phases connect at a temperature below which $J_3/J_1 = 0$ line separates (Ferro) and (Ferri) phases above $T_{c_q}$ with a second-order line and above the intersection point temperature of these three phases the upper wing of the second-order line with $J_3/J_1 > 0$ separates (Ferro) and (P) phases and the lower wing of the other second-order line $J_3/J_1 < 0$ separates the (Ferri) and (P) phases. Therefore, the point where these three phases coexist maybe called as a triple point of second-order type meaning that at this temperature the system can go either of these phases without need of any extra energy.

## REFERENCES


1. H. J. Elmers, *Int. J. Mod. Phys. B* **9**:3115 (1995).
2. *Digest 13th Int. Colloq. on Magnetic Films and Surfaces*, Glasgow (1991).
3. M. N. Baibich, J. M. Broto, A. Fert, F. Nguyen Van Dau, F. Petroff, P. Eitenne, G. Creuzet, A. Friederich, and J. Chazelas, *Phys. Rev. Lett.* **61**:2472; G. Binasch, P. Grunberg, F. Saurenbach, and W. Zinn, *Phys. Rev. B* 4828 (1989).
4. J. Sayama, T. Asahi, K. Mizutani, and T. Osaka, *J. Phys. D: Appl. Phys.* **37**:L1–L4 (2004).
5. R. Wu and A. J. Freeman, *Phys. Rev. B* **45**:7205 (1992); M. Donath, *J. Phys.: Condens. Matter* **11**:9421 (1999).
6. R. C. O'Handley and S. W. Sun, *Phys. Rev. Lett.* **66**:2798 (1991); G. Bochi, O. Song, and R. C. OòHandley, *Phys. Rev. B* **50**:2043 (1994).
7. Y. M. Seidov and G. R. Shaulov, *J. Phys.: Condens. Matter* **6**:9621 (1994); M. Jaščur and T. Kaneyoshi, *J. Magn. Magn. Mater* **168**:47 (1997); B. Laaboudi, M. Saber, and M. Kerouad, *Phys. Stat. Sol. (b)* **212**:153 (1999); T. Bouziane and A. Belaaraj, *Phys. Stat. Sol. (b)* **214**:387 (1999); T. Kaneyoshi and S. Shin, *Phys. Stat. Sol. (b)* **218**:537 (2000).
8. F. Dujardin, B. Stébé, A. Ainane, and M. Saber, *Chinese J. Phys.* **37**:479 (1999); T. Bouziane, *Phys. Stat. Sol. (b)* **217**:951 (2000); M. Bentaleb, N. El Aouad, and M. Saber, *Chinese J. Phys.* **40**:307 (2002).
9. G. Wiatrowski, G. Bayreuther, and K. Pruegl, *J. Mag. Magn. Mater.* **196–197**:26 (1999); G. Wiatrowski, *Physica A* **290**:107 (2001).
10. M. Bengrine, A. Benyoussef, H. Ez-Zahraouy, and F. Mhirech, *Physica A* **268**:149 (1999); H. Ez-Zahraouy and A. Kassou-Ou-Ali, *Chinese J. Phys.* **40**:86 (2002).
11. L. Bahmad, A. Benyoussef, and H. Ez-Zahraouy, *Surf. Sci.* **536**:114 (2003); X.-G. Wang, N.-N. Liu, S.-H. Pand, and G.-Z. Yang, *J. Magn. Magn. Mater.* **212**:121 (2000).
12. H. Ez-Zahraouy, L. Bahmad, and A. Benyoussef, *Physica A* **358**:86 (2005).
13. M. L. Lyra and C. R. da Silva, *Phys. Rev. B* **47**:526 (1993).
14. J. L. Monroe, *Physica A* **335**:563 (2004).
15. C.-K. Hu and N. Sh. Izmailian, *Phys. Rev. E* **59**:6489 (1999); E. Albayrak, *Phys. Stat. Sol. (b)* **244**:759 (2007).
16. L. Bahmad, A. Benyoussef, and H. Ez-Zahraouy, *J. Magn. Magn. Mater.* **251**:115 (2002); A. Benyoussef, H. Ez-Zahraouy, H. Mahboub, and M. J. Ouazzani, *Physica A* **326**:220 (2003).

17. J. W. Tucker, T. Balcerzak, M. Gzik, and A. Sukiennicki, *J. Magn. Magn. Mater.* **187**:381 (1998); M. Gzik-Szumiata and T. Balcerzak, *Acta Physica Slovaca* **48**:611 (1998).
18. L. Bahmad, A. Benyoussef, and H. Ez-Zahraouy, *Surf. Sci.* **552**:1 (2004); L. Bahmad, A. Benyoussef, and H. Ez-Zahraouy, *M. J. Condensed Matter* **5**:134 (2004).
19. E. Albayrak and O. Canko, *Physica A* **373**:363 (2007); O. Canko and E. Albayrak, *Phys. Rev. E* **75**:011116 (2007).
20. D. Gatteshi, O. Khan, J. S. Miller, and F. Palacio (eds.) *Magnetic Molecular Materials (NATO ASI Series)* (Dordrecht, Kluwer Academic, 1991); O. Khan, *Molecular Magnetism* (VCH Publishers, New York, 1993).
21. H. J. Williams, R. C. Sherwood, F. G. Foster, and E. M. Kelley, *J. Appl. Phys.* **28**:1181 (1957).
22. M. Bengrine, A. Benyoussef, A. El Kenz, M. Loulidi, and F. Mhirech, *J. Magn. Magn. Mater.* **183**:334 (1998).
23. K. Htoutou, A. Ainane, and M. Saber, *J. Magn. Magn. Mater.* **269**:245 (2004).
24. W. Jiang, G.-Z. Wei, and A. Du, *J. Magn. Magn. Mater* **250**:49 (2002).
25. W. Jiang and G.-Z. Wei, *Physica B* **362**:236 (2005).
26. M. Jaščur and T. Kaneyoshi, *J. Phys.: Condens. Matter* **5**:6313 (1993).
27. M. Bengrine, A. Benyoussef, A. El Kenz, and L. Peliti, *Physica B* **269**:34 (1999).
28. M. Jaščur and T. Kaneyoshi, *Physica A* **220**:542 (1995).
29. T. Kaneyoshi, *Phys. Rev. B* **52**:7304 (1995).
30. M. Jaščur and T. Kaneyoshi, *J. Phys. Condens. Mater.* **5**:6313 (1993).
31. M.-h. Yu and Z.-d. Zhang, *J. Magn. Magn. Mater.* **195**:514 (1999).
32. C.-K. Hu, N. Sh. Izmailian, and K. B. Oganesyan, *Phys. Rev. E* **59**:6489 (1999); E. Albayrak, S. Yilmaz, and S. Akkaya, *J. Magn. Magn. Mater* **310**:98 (2007).
33. P. J. Jensen, K. H. Bennemann, K. Baberschke, P. Poulopoulos, and M. Farle, *J. Appl. Phys.* **87**:6692 (2000).
34. B. Schmittmann and R. K. P. Zia, *Phys. Rep.* **301**:45 (1998).